Changes in the marine-terminating glaciers of east Greenland and potential connections to ocean circulation, 2000-2010

K. M. Walsh[1,2], I. M. Howat[1,2], Y. Ahn[2], E. M. Enderlin[1,2]

[1] School of Earth Sciences, The Ohio State University, Columbus, Ohio

[2] Byrd Polar Research Center, The Ohio State University, Columbus, Ohio

Abstract

Outlet glaciers on the periphery of the Greenland Ice Sheet have undergone substantial changes in the past decade. Limited geophysical observations of the marine-terminating glaciers of eastern Greenland's Geikie Plateau and Blosseville Coast suggest rapid rates of mass loss and short-term variability in ice dynamics since 2002. Glaciers in this region terminate into the Denmark Strait, which is an oceanographic transition zone between the Irminger and Greenland seas. We examine time series of thinning, retreat and flow speed of 38 marine-terminating glaciers along the central east Greenland coast from 2000 to 2010 and compare this record with coastal sea surface temperatures to investigate a potential relationship between warming of the sea surface and increased melt at the glacier termini. We find that glacial retreat, thinning and acceleration have been more pronounced throughout the Denmark Strait, supporting our hypothesis that ocean warming associated with shifts in the Irminger and East Greenland currents are causing increased melt at the ice-ocean interface.

1. Introduction

Multiple studies using a range of methods show that mass loss in Greenland is due to both increased surface melting and discharge from marine-terminating outlets, with the most pronounced glacier change being observed in the southeast and northwest quadrants (Luthcke et al., 2006; Velicogna and Wahr, 2006; Velicogna, 2009; van den Broeke, 2009). Rapid, unpredicted changes in the dynamics of fast-flowing outlet glaciers draining the periphery of ice sheets have lead to increased rates of mass loss (e.g., Krabill et al., 1999; Krabil et al., 2004;

Tapley et al., 2004; Luthcke et al., 2006; Rignot and Kanagaratnam, 2006; Thomas et al., 2006; Pritchard et al., 2009).

Previous studies have linked recent increases in mass loss to changes in ocean (e.g., Holland et al., 2008; Hanna et al., 2009; Straneo et al., 2010) and atmospheric circulation (Box et al., 2006; Zwally et al., 2011). The observed speed-up of outlet glaciers in southeast Greenland in the early 2000's coincided with the onset of a warming trend in the subpolar North Atlantic Ocean (Bersch et al., 2007; Myers et al., 2007; Thierry and Mercier, 2008; Straneo et al., 2010). Additionally, abrupt warming of subsurface ocean temperatures in 1997 along Greenland's west coast has been linked to increased thinning and retreat of Jakobshavn Isbræ, likely initiated by the influx of warmer water originating in the Irminger Sea off the southeast coast of Greenland (Holland et al., 2008; Hanna et al., 2009).

It is possible that warming of the ocean surrounding the Greenland Ice Sheet is increasing melt and retreat of the ice sheet's outlet glaciers, with a potential link to atmospheric warming (Box et al., 2009; Christofferson et al., 2011). Although the mechanisms driving the circulation of warmer North Atlantic waters are not well understood (e.g., Straneo et al., 2010), one hypothesis is that increased glacier runoff promotes convection of deep, warm fjord water through entrainment of relatively warm ocean water with more buoyant subglacial meltwater plumes, increasing melt rates at the calving front (Motyka et al. 2003; Rignot et al. 2010). Increased melt has been observed through limited *in situ* measurements at the ice-ocean interface throughout the last decade, with the temperature and renewal rates of ocean water suggesting that this water is causing increased submarine melting at the margin of the ice sheet (Thomas, 2004; Nick et al., 2009; Straneo et al., 2010; Seale et al., 2011). Recent oceanographic studies have demonstrated that although subtropical ocean waters reach glacier fjords in southeast Greenland, there is ultimately no proof that it comes into direct contact with glaciers. Alternatively, Straneo et al. (2010) indicated that warming of North Atlantic subsurface water itself could increase melt and calving rates. A recent study by Seale et al., 2011, suggests that warming of the North Atlantic via subtropical water transport by the Irminger Current may be causing increased inter-annual melt rates in east Greenland glaciers south of 69°N, with limited to no inter-annual glacier change occurring north of that latitude.

Numerous, large marine-terminating outlet glaciers drain the central-eastern part of the Greenland coast from roughly 66°N to 71°N latitude, including the Geikie Plateau and Blosseville Coast regions (Figure 1). This region includes the thermodynamic transition zone from the Irminger Sea into the Greenland Sea through the Denmark Strait, spanning from roughly 66°N to 69°N. Contrasting patterns of glacial change spanning the length of the Denmark Strait would provide further evidence that changes in the circulation of the Irminger Sea (i.e., a potential increase in the transport of subtropical waters) are causing accelerated melt of the marine-terminating outlet glaciers in southeast Greenland.

This study uses satellite measurements to observe changes of 38 marine-terminating glaciers wider than 2-km in east Greenland between ~65˚34'N to ~71˚53' N over the past decade. From these data, we identify differences in behavior between glaciers north and south of the Denmark Strait's northern limit (~69˚N) to test the hypothesis that such behavior is directly associated with variable inflow of subtropical waters from the Atlantic Ocean. This study attempts to corroborate results by Seale et al., 2011, which suggested that a disparity in inter-annual glacier behavior north and south of 69°N may be caused by warm subsurface ocean conditions south of 69°N, by examining more glaciers near this oceanographic transition zone using imagery with a higher spatial resolution. Additionally, we assess the importance of the other mechanisms of glacier change in this region, such as surging and variability in dynamic thinning.

2. Data Sources and Methods

Data acquired from 2000 to 2010 over the Geikie Plateau and Blosseville Coast regions include visible and near-infrared (VNIR) bands of the Advanced Spaceborne Thermal Emission Reflector and Radiometer (ASTER) and the panchromatic band of the Landsat-7 Enhanced Thematic Mapper Plus (Landsat-7 ETM+) sensor for creating time series of front position, flow speed, and elevation change (from ASTER digital elevation models). Sea surface temperatures were derived from data collected by the Moderate Resolution Imaging Spectroradiometer (MODIS) instrument.

Imagery from the Landsat-7 ETM+ satellite was obtained from the United States Geological Survey (USGS) Global Visualization Viewer (GLOVIS, http://glovis.usgs.gov) public archive. Mostly cloud-free images from the panchromatic band were selected to create image mosaics of the area for each year of the study period. The data have a 16-day repeat pass cycle and have a pixel resolution of 15 m. Orthorectified images and digital elevation models (DEMs) from ASTER were collected from the USGS Land Processes Data Active Archive Center (LP DAAC, https://lpdaac.usgs.gov), including images that were cloud-free or partially clouded in order to quantify thinning rates with minimal error. ASTER's host satellite, Terra, has a 16-day repeat pass cycle but images are only acquired on-demand, so that few images are available for a given glacier each melt season (Joughin et al., 2008). DEMs were created using nadir and backward-looking VNIR image pairs acquired 57 seconds apart. Relative DEMs were produced without ground control and were later registered using offsets over off-ice terrain (i.e., stationary bedrock). Following this correction, DEM vertical accuracy is better than 10 m over glacier ice.

MODIS Sea Surface Temperatures (SSTs) were obtained from the Physical Oceanography Distributed Active Archive Center (PODAAC, http://podaac.jpl.nasa.gov). Identical MODIS instrument are onboard two NASA Earth Observing System (EOS) satellites, Terra and Aqua, making MODIS capable of covering the entire surface of the Earth twice daily. SSTs were determined using an algorithm described by Armstrong (2002), and have an accuracy of ± 0.25°C.

2.1 Front Positions

Front positions for each glacier were manually digitized from Landsat-7 ETM+ and ASTER images using two methods of measurement: first, a polygon-vector method (e.g., Moon and Joughin, 2008; McFadden et al., 2011) was used to measure changes in the near-terminus area, and second, a centerline method which measures the intersection of the ice front with the central flow line of the glacier. The polygon-vector method accounts for asymmetric variations in front shape of each glacier, as front position vector tracings give information on net area change of each glacier, but this method is time-consuming and inaccurate when the front is only partially visible. The centerline method, in contrast, is a less time-consuming process and measurements can be made even when the front is partially obscured by clouds, but this method only captures variability at a single point along the front. In order to test the sensitivity of our results to either method, we mapped the fronts of 3 glaciers using both methods for comparison (Midgard, Kangerdlugssuaq, Sortebrae). These two methods yield very similar results, normally only a distance of ± 0.1 km apart (which is included in the measurement error of approximately 0.1 km). We therefore used the more efficient centerline method to generate our dataset.

2.2 Surface Elevations

Transects were drawn along the central flow line from sea level to the accumulation zone on the first Landsat-7 ETM+ image for each glacier (usually from 1999), and this transect information was transferred to the ASTER DEM subsets. Elevation profiles along these transects were generated for each glacier to quantify thinning. Individual elevation profiles were manually edited for errors resulting from clouds and failure of the DEM generation software (and subsequent generation of spurious elevation data). The data were then vertically registered by subtracting offsets over ice-free terrain. Multiple elevations for a given year were averaged together to give a single elevation profile for each year in the time series.

2.3 Surface Speeds

We extracted glacier surface speeds from ASTER and Landsat image pairs using the IMMATCH/MIMC Repeat Image Feature Tracking (RIFT) software distributed by the Glacier Dynamics Group at The Ohio State University. This method of feature tracking utilizes pairs of Landsat-7 ETM+ and ASTER VNIR images collected between 10-90 days apart. A detailed description of the software, including a full error assessment and validation, is given in Ahn and Howat, in press and a brief description is in Howat et al., 2010. Here we examine a time series of average surface speeds taken from a point along the centerline approximately 10 km from the most retreated front position of each glacier. Error in this method varies with pixel resolution and time between image pairs, and are less than 1 m d^{-1} for the data used in this study (Ahn and Howat, in press).

3. Results

We find a wide range in glacier behavior across our study area over the past decade. In general, our results support the findings of Seale et al., 2011, which suggested that a strong contrast in inter-annual glacier behavior north and south of 69°N may be caused by warm subsurface ocean conditions south of 69°N. A greater magnitude of change, especially in extent of front retreat, occurred on the glaciers terminating along the Blosseville Coast and Kong Christian IX Land coast, supporting the hypothesis that warming of Greenland's coastal waters is the primary trigger for change. In contrast, we find little change occurred on the glaciers on the northern portion of the Geikie Plateau. Our results are presented in detail below.

3.1 Overview of Front Position Changes

All 38 glaciers retreated between 2000 and 2010, but the magnitude of retreat was highly variable, ranging from ≤ 0.1 km to 9 km. The mean retreat for all 38 glaciers over the time period was 1.6 km, with the largest change observed to be 9.193 km from 2000 to 2010 (Midgard Glacier). Greater front retreat is found along the Blosseville Coast and Kong Christian Ix Land coastline, with 14 of the 25 glaciers in this area retreating >1.0 km over the time period. The mean total retreat of glaciers in this region of the study area was 2.1 km, while the mean total retreat of glaciers terminating into Scoresby Sound and Gasefjord (inner Scoresby Sound) and further north was < 0.5 km. The large retreats of a few glaciers, however, skew the mean front retreat; the median retreat for all 38 glaciers in the study area is only 0.94 km. Nearly half of the glaciers retreated 1.0 kilometer or more during the time period. Figure 2 shows total front change for each glacier as the difference in front position from 2000 to 2010.

3.2 Overview of Surface Elevation Changes

Surface elevation changes were much more variable and not as spatially consistent as changes in front position. We observe generally no change on the glaciers terminating into Scoresby Sound and its channels north of the eastern-most point of the Geikie Plateau peninsula (70°9'N, 22°3'W). For glaciers south of 70°9'N, rates of thinning 15-km inland of the front varied from ≥ 10 m of thinning to roughly 155 m of thinning between 2000 and 2010. For glaciers north of 70°9'N, thinning rates varied from approximately 10 m of thickening to 35 m of thinning between 2000 and 2010. Only two glaciers thickened over the study period, on the order of 5-7 m of thickening at 15 km inland from the termini, both of which were located north of 70°9'N. Figure 3 shows thinning evident 15 km inland of the terminus for each glacier as the difference in surface elevation from 2000 to 2010. Figure 4 shows annual elevation profiles for the six glaciers discussed in detail below.

3.3 Overview of Surface Speed Changes

Surface speeds varied both spatially and temporally, with the highest speeds measured on Kangerdlugssuaq and Helheim glaciers during periods of acceleration between 2005 and 2006 (e.g., Howat et al., 2008a; Joughin et al., 2008; Luckman et al., 2006). Many of the glaciers in this study exhibit seasonal variability in surface speed, oscillating on the order of ± 7 m per year, especially in the Scoresby Sound region north of the Geikie Plateau. For example, Daugaard-Jensen Gletscher had speeds varying annually by 25% between 7.5 and 11 m d^{-1}, while Rolige Brae had surface speeds varying seasonally between 6 m d^{-1} in the summer to near stagnation in the winter. Kangerdlugssuaq Glacier displayed the largest range in its surface speed as a result of its sustained acceleration between 2004 and 2006, accelerating from 10 m d^{-1} to 27 m d^{-1}. Maximum surface speeds occurred in the summer for all glaciers, with a mean maximum summer surface speed of 7.5 m d^{-1} for all glaciers in the study. Figure 5 shows average surface speeds for all glaciers in the study area.

3.4 Spatial Patterns of Glacier Change

Here we discuss differences in glacier change between the three major subregions of the study area, with several glaciers discussed in detail to highlight regionally representative behavior. The regions are presented from south to north.

3.4.1 Kong Christian IX Land (Sermilik Fjord to Kangerdlugssuaq Fjord)

This area underwent the greatest magnitude of change in dynamics (i.e., front retreat, thinning, surface speed), particularly in the magnitude of front retreat. These glaciers drain directly from the Greenland Ice Sheet. Peak rates of front change occurred between 2003 and 2005, suggesting a regional forcing that was at a maximum during this time. The mean front retreat of glaciers in this subset was 2.9 km, and the median front retreat was 1.6 km. The average thinning observed 15-km inland of the glacier terminus was 28 m, and the elevation profiles for roughly half of these glaciers show evidence of extensive thinning (i.e., mean thinning at 15 km from the glacier terminus >30 m). The mean maximum surface speed was 8.8 m d^{-1}, with a median maximum surface speed of 7.7 m d^{-1}. All maximum surface speeds occurred in the summer months.

Midgard Glacier, which terminates into the long northeast channel of Sermilik Fjord, underwent the largest magnitude of change in front position, thinning, and surface speed of the glaciers sampled (Figure 6). Sustained, inter-annual retreat of Midgard increased in 2003, with a pronounced pattern of seasonal advance-and-retreat lasting through 2007. Between early 2008 and late 2009, the glacier retreated 4.0 km before a brief period of re-advance in late 2009/early 2010 and an additional retreat of 1.5 km. The most significant thinning occurred below 1000 m a.s.l. elevation and within 40 km of the terminus; the glacier thinned roughly 100 m from 2000 to 2010 at 10 km from the terminus, decreasing up-glacier. This rate of thinning was consistent with the pattern of front retreat throughout the time series, with an overall acceleration in both front retreat and thinning occurring in late 2007 into 2008. Surface speeds increased from roughly 4 m d^{-1} in 2000 to 9 m d^{-1} in 2009 at a center point roughly 5 km up-glacier from the glacier's most retreated position.

3.4.2 Blosseville Coast

The glaciers along the Blosseville Coast display the highest degree of variability in changes in front position, thinning, and surface speed. While most glaciers underwent substantial change, there was no clear temporal or spatial pattern. On average, glaciers in this region retreated by 1.6 km, with a median retreat of 0.9 km and a median thinning of 22 m at 15-km inland of the front. Thinning rates were highly variable, with dynamic thinning evident on 2 of the 14 glaciers in this area as suggested by rapid acceleration followed by extensive thinning and stretching originating at the front, including the extreme thinning observed on Kangerdlugssuaq (160 m). The mean (median) maximum surface speed was 7.4 m d^{-1} (5.9 m d^{-1}). All maximum surface speeds occurred in June or July.

Kangerdlugssuaq and Frederiksborg are examples of two glaciers in close proximity to one another that display contrasting behavior. Kangerdlugssuaq is ~9 km wide and terminates into a 40-km long fjord (Figure 7). Several studies have documented the large, inter-annual retreat, acceleration and thinning of Kangerdlugssuaq (e.g., Luckman et al., 2006; Howat et al., 2007, 2011). This glacier's front oscillated seasonally by almost 2 km between 2000 and 2004. Between late 2004 and early 2006, Kangerdlugssuaq retreated roughly 5 km. During retreat, the glacier accelerated from roughly 12 m d^{-1} in 2000 to 27 m d^{-1} in 2006 and thinned more than 150 m near the front. Thinning propagated up-glacier following the period of acceleration. Kangerdlugssuaq surface speeds slowed following the 2005-2006 acceleration, and the glacier re-advanced or thickened so that the front of the glacier remains approximately 7 km from its initial position in 2000.

Frederiksborg is a much narrower glacier, terminating at two calving fronts into the same fjord as Kangerdlugssuaq. Frederiksborg retreated roughly 1.5 km from 2000 to 2004, and has maintained a steady pattern of 0.7-km seasonal retreat and advance since 2005. This glacier had negligible elevation change from 2000 to 2009. In 2010, however, the glacier thickened significantly at a location approximately 10-km from the front (no elevation data available closer to the front in 2010). Surface speeds for this glacier were relatively stable from 2000 to 2006, varying between 3 and 5 m d^{-1}, with no observed seasonality. Beginning in 2007, however, the glacier began to show a large seasonal cycle in surface speeds, from near stagnation in the winter to 13 m d^{-1} in mid-summer, coinciding with the large seasonal variation in front position.

Several glaciers in this region have been previously identified as surging glaciers, with two examples evident in this study (Sortebrae and Johan Petersen Bugt). Sortebrae (68°44'N, 26°59'W) is a surge-type glacier (e.g., Jiskoot et al., 2001; Jiskoot and Juhlin, 2009) that has a large central trunk with smaller subsidiary glaciers occupying several channels on the south facing side of the Geikie Plateau. Sortebrae retreated steadily at roughly 500 m per year from 2000 to 2010. Consistent with this steady retreat, the glacier thinned 60 m within 15 km of its front with no resolvable thinning above. Since this glacier is in a quiescent period of surge behavior (Jiskoot et al., 2001; Murray et al., 2002) surface speeds were relatively slow, ranging from near stagnation to 3 m d^{-1}, with slight seasonality.

3.4.3 Scoresby Sound and Gasefjord

The glaciers terminating into and north of Scoresby Sound exhibited relatively little change in front position, thinning, and surface speed. The mean (median) front retreat of glaciers in this subset was 0.51 km (0.32 km) with strong seasonal variations in front position and speed. The mean (median) maximum surface speed was 6.6 m d^{-1} (5.3 m d^{-1}). The strong seasonal signal in front change observed in this region is typified by Daugaard-Jensen Gletscher, which undergoes a seasonal oscillation in front position of ~1 km annually. Its inter-annual mean front position, however, has not changed since 2000. The glacier thinned approximately 30 m below 400 m elevation, with negligible thinning at higher elevations. Daugaard-Jensen Gletscher was the fastest moving glacier observed in the Scoresby Sound region, with a maximum speed of 11 m d^{-1} in June 2006 and a strong seasonal pattern of acceleration and deceleration generally following the cyclic pattern of front advance and retreat.

4. Discussion

Changes in the front positions, surface elevations, and surface speeds of 38 marine-terminating glaciers in central east Greenland indicate that glaciers in Kong Christian IX Land and the Blosseville coast, which terminate into the Denmark Strait, thinned and retreated more extensively than glaciers north of the Denmark Strait, suggesting a relationship between changes in circulation of the Irminger Sea and enhanced melt of glaciers in southeast Greenland. The ten outlet glaciers on the coast from Sermilik Fjord to Kangerdlugssuaq fjords all underwent accelerated retreat following 2003, a year of anomalously high air and sea surface temperatures along the southeast Greenland coast (Howat et al., 2008a). Additionally, it is possible that a distinct change in accumulation and ablation rates north of 71°N is causing glacial mass loss to be occurring at a lesser rate in the Scoresby Sound and Gasefjord region (e.g., Box et al., 2006; Zwally et al., 2011). While there is a clear latitudinal distinction between the magnitudes of change, the relative magnitudes of thinning and retreat varied substantially from glacier to glacier. The discussion presented below focuses on the contribution of surging to regional glacier change and the effects of dynamic thinning on glaciers in this region, particularly south of Kangerdlugssuaq Fjord. Additionally, the discussion will outline the relationship between sea surface temperatures and magnitude of glacier change, including the use of sea surface temperatures as a proxy for ocean circulation patterns.

4.1 Surging Glaciers in East Greenland

Several tidewater glaciers in east Greenland have exhibited surge-like flow speed behavior, with a majority experiencing surging similar to glaciers in Svalbard (e.g., Jiskoot and Juhlin, 2009), and morphological attributes commonly attributed to glacial surges (Murray et al., 2002; Jiskoot et al., 2003). Glacial surges are events of varying time scales where a glacier rapidly accelerates over several months and decelerates gradually due to a sudden release of trapped subglacial water. Svalbard-type surging can be identified on glaciers that experience “multi-phase surges” and accelerate over the course of several months, followed by a deceleration period of approximately 6-7 years before establishing a quiescent period of at least 60 years (Jiskoot and Juhlin, 2009). A glacial surge follows a quiescent period of slow retreat, which can vary from years to decades. Several means exist to identify "surging" glaciers, including warped moraine shapes, sheared-off ice tributaries, varying crevasse patterns, and rougher-than-usual glacial surfaces (Jiskoot et al., 2003). Alaskan-type surging (which occurs at a much more rapid pace than Svalbard-type surging and allows for shorter quiescent phases (e.g., Jiskoot and Juhlin, 2009)) has been documented on Sortebrae (68°44'N, 26°59'W), which surged for roughly 19-35 months from 1992 to 1995 following a quiescent phase of between 39-49 years. Ice flow during the surge event increased by up to 60-1500 times over the glacier's quiescent-phase speeds and was sustained at rates of up to 30 m d^{-1} for more than 12 months (Murray et al., 2002). While Sortebrae is the only glacier in central east Greenland where active, rapid Alaskan-type surging has been recently observed, other studies (e.g., Weidick, 1988; Jiskoot et al., 2003; Jiskoot and Juhlin, 2009) have identified morphological signs of Svalbard-type surging on other glaciers in this region, including Dendrit and Borggraven glaciers along the Blosseville Coast, which indicates that Svalbard-type surging is a regional mechanism for glacier change.

4.2 Glacier Thinning

In addition to remotely sensed observations, ice flow models suggest that marine terminating glaciers are sensitive to changes at the ice front and hydraulic basal conditions, leading to dynamic instabilities and thinning (Nick et al., 2009). Dynamic thinning occurs when perturbations in glacier stresses at the calving front propagate up-glacier, causing acceleration and thinning to migrate inland (Joughin et al., 2008; Nick et al., 2009). Dynamic thinning is the primary cause of observed thinning for marine-terminating outlet glaciers along the northwest and southeast margins of the Greenland Ice Sheet (Abdalati et al., 2001; Krabill et al., 2004; Howat et al., 2005; Pritchard et al., 2009).

Dynamic thinning has been observed on several glaciers in southeast Greenland, including Kangerdlugssuaq, where dynamic thinning is detectable from the glacier's terminus to approximately 100 km inland (Pritchard et al., 2009). Our observations suggest that roughly half of the glaciers between Sermilik and Kangerdlugssuaq fjords are experiencing rapid dynamic thinning as well, with the most dramatic example being Midgard Glacier. From the glacier's elevation profile, it is apparent that thinning began near the front of the glacier at the beginning of the time series and has since propagated at least 45-km inland (see Figure 4). In our study region, dynamic thinning is mostly confined to the south of Kangerdlugssuaq, where mean and median surface speeds are the highest. Thus, it is likely that the smaller outlet glaciers to the south of Kangerdlugssuaq are contributing a considerable amount of the mass loss measured from southeast Greenland as previously discussed in Howat et al. (2008b). This could explain the continued high rates of mass loss observed by GRACE in the southeast, despite decreased rates of loss at Kangerdlugssuaq, and mass gain at Helheim (Howat et al., 2011).

4.3 Oceanographic Forcing of Glacier Melt

Limited studies of the subsurface ocean conditions of the North Atlantic surrounding southeast Greenland reveal a gradual increase in temperatures of Irminger Sea from 2003 to 2004, which coincided with this regional acceleration of glaciers in southeast Greenland (Straneo et al., 2010; Myers et al., 2007; Bersch et al., 2007; Thierry et al., 2008). Examination of oceanographic data collected in the fjords and on the continental shelf near three of Greenland's largest glaciers, including Kangerdlugssuaq and Helheim on the east coast and Jakobshavn Isbræ on the west coast, suggests that changes in oceanographic conditions may be capable of triggering major changes at the termini of Greenland's marine terminating glaciers (e.g., Holland et al., 2008; Straneo et al., 2010). Holland and others (2008) documented a sudden increase in ocean temperatures along the west coast of Greenland in 1997 that corresponded with rapid thinning at Jakobshavn Isbræ, a glacier that had been slowly thickening and decelerating throughout the 1990s. Before 1997, Jakobshavn Isbræ terminated into a 15-km long floating ice tongue. A sudden increase in the temperature (measured in this MODIS SST dataset) of the fjord water could explain the roughly 80 m yr^{-1} of thinning that occurred between 1997 and 2001, and the disintegration of the glacier's floating tongue soon after (Motyka et al., 2011; Holland et al., 2008).

Although changes in oceanographic forcing coincided with the retreat of Jakobshavn Isbræ (e.g., Holland et al., 2008), widespread measurements of subsurface ocean conditions are not readily available and sea surface temperatures (SSTs) may not be a reasonable proxy for subsurface ocean temperatures for most Greenland outlet glaciers (e.g., Straneo et al., 2010). However, the data derived from MODIS used in this study show a clear increase in SSTs in late 2003 at the southern-most study site (SST-A), which is roughly 80 km south of the mouth of Sermilik Fjord and 140 km south of the terminus of Helheim Glacier. Temperatures at this location increased from 6°C in late 2002 to 9.5°C in late 2003. Two other SST-observation sites, SST-B and SST-C, also show a slight increase in temperature from 2002 to 2003. Additionally, the temperature at SST-A appears to have increased in late 2010 although not as dramatically as in 2003, so continued monitoring of the glaciers in southeast Greenland is necessary to see if another regional glacier change event has been initiated. The two northern-most points chosen to observe SSTs do not contain the spike in temperature in 2003 or in 2010 as shown in Figure 8. This spike in SSTs at the southern-most measuring point in 2003 in addition to the anomalously warm air temperatures observed in southeast Greenland at this time may have been the impetus for the glacier dynamics change on the Kong Christian IX Land coast from 2003 to 2005. Definitive conclusions cannot be drawn from this increase in sea surface temperatures and subsequent acceleration and thinning of southeast Greenland's marine-terminating glaciers, although the connection between ice and ocean dynamics is evident in this study and in previously published results (e.g., Holland et al., 2008; Howat et al., 2008a; Straneo et al., 2010; Murray et al., 2010).

5. Conclusions

Our analysis of changes in 38 marine-terminating glaciers in the Geikie Plateau and Blosseville Coast regions of Greenland's central east coast over the past decade reveal widespread retreat and acceleration in southeast Greenland up to the Denmark Strait and little inter-annual change further north. This pattern suggests that accelerated melt and calving in southeast Greenland is linked to changes in the circulation of the Irminger Sea, which supports the findings of Seale et al., 2011 by providing a closer look at a larger number of glaciers in the Denmark Strait region. In addition, glaciers terminating in fjords near the Denmark Strait were more synchronous in their behavior, while glaciers north of the Denmark Strait were more variable, which also indicates that a regional forcing may be behind glacier acceleration and melt in this region.

Our initial hypothesis stated that, if ocean warming is driving glacier change, there would be a more pronounced changes in front position, elevation, and ice speed on glaciers south of Kangerdlugssuaq Fjord and south-facing glaciers of the Blosseville Coast compared to north-facing glaciers of the Geikie Plateau as a result of exposure to the warming of the North Atlantic and its associated coastal currents. While this analysis suggests that oceanographic forcing may be affecting glacier melt through the Denmark Strait, observations of glaciers in this region and of the surrounding ocean are still too limited to state definitively that changing ocean dynamics are the sole regional forcing affecting glacier change in this region. Future studies are required that incorporate ocean monitoring stations near the outlet glaciers lining the Blosseville Coast and along the coast from Sermilik Fjord to Kangerdlugssuaq Fjord in order to obtain more information about the subsurface oceanographic conditions along the continental shelf and closer to outlet glacier termini.

The methods used in this study to quantify glacier change in central east Greenland can be applied to other areas where outlet glaciers are being assessed for ongoing changes in front position, surface elevation, and surface speed. However, the methods and imagery used in this analysis have limitations. The east Greenland coast is often obscured with clouds for much of the year, making it difficult to have a complete time series of Landsat-7 ETM+ or ASTER imagery over a particular location. Future studies should incorporate all-weather and all-year synthetic aperture radar data and high-resolution commercial satellite imagery to provide a much more complete picture of change. Additionally, elevation data collected by airborne laser altimetry acquired as part of NASA's Operation IceBridge initiative will provide a sufficient alternative to using moderate resolution ASTER digital elevation models for measuring changes in glacier surface elevation.

Using a wide and growing array of airborne and satellite remote sensing platforms, observations and measurements of the continued mass loss and glacier change on the Greenland Ice Sheet are becoming more abundant and accessible for studying the effects of a warming climate on the ice sheet. Mass loss is occurring at accelerated rates on marine-terminating glaciers in the southeast drainage areas of the ice sheet, as shown by gravity anomalies, altimetry data, and imagery showing loss at glacier termini. The implications of melting glaciers in Greenland are global in scope; ongoing changes in ice cover are expected to continue contributing to changes in sea level, which is one of the greatest challenges facing coastal communities and heavily populated coastal urban centers. These areas of extreme glacier change discussed in this analysis indicate that continuous monitoring of both local glacier and ice sheet changes are necessary to develop a better understanding of how the Greenland Ice Sheet is adjusting to atmospheric and oceanographic changes.

6. Acknowledgements

This work was made possible by NASA grant NNX08AQ83G, awarded to I. Howat. The RADARSAT image in figures 1 and 2 was provided by I. Joughin.

7. References

Abdalati, W., Krabill, W., Frederick, E., Manizade, S., Martin, C., Sonntag, J., Swift, R., Thomas, R., Wright, W., and Yungel, J., (2001), Outlet glacier and margin elevation changes: Near-coastal thinning of the Greenland ice sheet, *J. Geophys. Res*., **106**(D24), 729-733.

Ahn, Y. and I. Howat (in press), Efficient, Automated Glacier Surface Velocity Measurement from Repeat Images Using Multi-Image/Multi-Chip (MIMC) and Null Exclusion Feature Tracking, *IEEE Trans. on Geoscience and Remote Sensing.*

Armstrong, E. (2002), MODIS Sea Surface Temperature (SST) Products, *Rep. CL 02-0691*, Jet Propul. Lab., Pasadena, Calif. (Available from http://podaac.jpl.nasa.gov/pub/documents/dataset_docs/modis_sst.html)

Cazenave, A, and Nerem, R.S., (2004), Present day sea level change: Observations and causes, *Rev. Geophysics*, **42**(3), 1-20.

Bersch, M., Yashayaev, I., and Koltermann, K. P., (2007), Recent changes of the thermohaline circulation in the Subpolar North Atlantic, *Ocean Dyn*., **57**, 223-235.

Box, J., Yang, L., Bromwich, D., and Bai, L., (2009), Greenland Ice Sheet Surface Air Temperature Variability: 1840–2007, *J. Climate*, **22**, 4029–4049.

Box, J., Bromwich, D., Veenhuis, B., Bai, L., Stroeve, J., Rogers, J., Steffen, K., Haran, T., Wang, S., (2006), Greenland Ice Sheet Surface Mass Balance Variability (1988-2004) from Calibrated Polar MM5 Output, *J. Clim.,* **19**, 2873-2800.

Chen, J., Wilson, C., and Tapley, B., (2006), Satellite gravity measurements confirm accelerated melting of Greenland ice sheet, *Science,* **311**, 1754.

Christoffersen, P., Mugford, R.I, Heywood, K.J, Joughin, I., Dowdeswell, J.A., Syvitski, J.P.M, Luckman, A., and Benham, T.J., (2011), Warming of waters in an East Greenland fjord prior to glacier retreat: mechanisms and connection to large-scale atmospheric conditions, *The Cryosphere*, **5**, 701-714.

Dowdeswell, J. (2006), The Greenland ice sheet and sea level rise, Science, **311**: 963-964.

Hamilton, G. (1992), Investigation of surge-type glaciers in Svalbard. (Ph.D. thesis, University of Cambridge).

Hanna, E., Cappelen, J., Fettweis, X., Huybrechts, P., Luckman, A., and Ribergaard, M.H., (2009), Hydrologic response of the Greenland ice sheet: the role of oceanographic warming, *Hydrol. Process*., **23**, 7-30.

Hanna, E., Huybrechts, P., Steffen, K., Cappelen, J., Huff, R., Shuman, C., Irvine-Finn, T., Wise, S., and Griffiths, M., (2008), Increased runoff from melt from the Greenland ice sheet: A response to global warming, *J. Clim*., **21**, 331-341.

Hanna, E., and Braithwaite, R., (2003), The Greenland ice sheet: a global warming signal? *Weather*, **58**, 351-357.

Holland, D., Thomas, R., De Young, B., Ribergaard, M.H., and Lyberth, B., (2008), Acceleration of Jakobshavn Isbrae triggered by warm subsurface ocean water, *Nature Geosci.,* **1**, 659-664.

Howat, I., Ahn, Y., Joughin, I., van den Broeke, M., Lenaerts, J., and Smith, B., (2011), Mass balance of Greenland's three largest outlet glaciers, 2000-2010, *Geophys. Res. Lett.,* **38**, L12501.

Howat, I., Box, J.E., Ahn, Y., Herrington, A., and McFadden, E.M., (2010), Seasonal variability in the dynamics of marine-terminating outlet glaciers in Greenland, *J. Glac*., **56**(198), 601-613.

Howat, I., Joughin, I., Fahnestock, M., Smith, B., and Scambos, T., (2008a), Synchronous retreat and acceleration of southeast Greenland outlet glaciers 2000-2006: ice dynamics and coupling to climate, *J. Glac*., **54**(187), 646-660.

Howat, I., Smith, B., Joughin, I., and Scambos, T., (2008b), Rates of southeast Greenland ice volume loss from combined IceSAT and ASTER observations, *Geophys. Res. Lett*., **35**, L17505.

Howat, I., Joughin, I., and Scambos, T., (2007), Rapid Changes in Ice Discharge from Greenland Outlet Glaciers, *Science*, **315**, 1559.

Howat, I., Joughin, I., Tulaczyk, S., and Gogineni, S., (2005), Rapid retreat and acceleration of Helheim Glacier, east Greenland, *Geophys. Res. Lett*., **32**, L22502.

Jiskoot, H. and Juhlin, D., (2009), Surge of a small East Greenland glacier, 2001-2007, suggest Svalbard-type surge mechanism, *J. Glaciol*., **55**(191), 567-570.

Jiskoot, H., Murray, T., and Luckman, A., (2003), Surge potential and drainage-basin characteristics in East Greenland, *Ann. Glac*., **36**(1).

Jiskoot, H., Pedersen, A.K., and Murray, T., (2001), Multi-model photogrammetric analysis of the 1990s surge of Sortebrae, East Greenland, *J. Glaciol.* **47**(159), 677-687.

Joughin, I., Smith, B., Howat, I., Scambos, T., and Moon, T., (2010), Greenland flow variability from ice-sheet-wide velocity mapping, *J. Glac*., **56**(197), 415-429.

Joughin, I., Howat, I., Alley, R.B., Ekstrom, G., Fahnestock, M., Moon, T., Nettles, M., Truffer, M., and Tsai, V.C., (2008), Ice-front variation and tidewater behavior on Helheim and Kangerdlugssuaq Glaciers, Greenland, *J. Geophys. Res*., **113**, F01004.

Joughin, I. (2002), Ice-sheet velocity mapping: a combined interferometric and speckle-tracking approach, *Ann. Glac*., **34**(1), 195-201.

Kamb, B., (1987), Glacier surge mechanism based on linked cavity configuration of the basal water conduit system, *J. Geophys. Res.*, **92**.

Krabill, W., Hanna, E., Huybrechts, P., Abdalati, W., Cappelen, J., Csatho, B., Frederick, E., Manizade, S., Martin, C., Sonntag, J., Swift, R., Thomas, R., Yungel, J., (2004), Greenland Ice Sheet: Increased coastal thinning, *Geophys. Res. Lett*., **31**, L24402.

Krabill, W., Frederick, E., Manizade, S., Martin, C., Sonntag, J., Swift, R., Thomas, R., Wright, W., and Yungel, J., (1999), Rapid Thinning of Parts of the Southern Greenland Ice Sheet, *Science,* **283**, 1522-1524.

Luckman, A., Murray, T., de Lange, R., and Hanna, E.,(2006), Rapid and synchronous ice-dynamic changes in East Greenland, *Geophys. Res. Lett*., **33**, L035035.

Luthcke, S., Zwally, H.J., Abdalati, W., Rowlands, D.D., Ray, R.D., Nerem, R.S., Lemoine, F.G., McCarthy, J.J., and Chinn, D.S., (2006), Recent Greenland mass loss by drainage system from satellite gravity observations, *Science*, **314**, 1286-1289.

McFadden, E., Howat, I., Joughin, I., Smith, B., and Ahn, Y., (2011), Changes in the dynamics of marine terminating outlet glaciers in west Greenland (2000-2009), *J. Geophys. Res*., **116**, F02022.

Meier, M., and Post, A., (1987), Fast tidewater glaciers, *J. Geophys. Res*., **92**(B9), 9051-9058.

Moon, T., and Joughin, I., (2008), Changes in ice front position on Greenland's outlet glaciers from 1992 to 2007, *J. Geophys. Res*., **113**, F02022.

Motyka, R., Truffer, M., Fahnestock, M., Mortensen, J., Rysgaard, S., and Howat, I., (2011), Submarine melting of the 1985 Jakobshavn Isbrae floating tongue and the triggering of the current retreat, *J. Geophys. Res*., **116**, F01007.

Murray, T., Scharrer, K., James, T.D., Dye, S.R., Hanna, E., Booth, A.D., Selmes, N., Luckman, A., Hughes, A.L.C., Cook, S., and Huybrechts, P., (2010), Ocean regulation hypothesis for glacier dynamics in southeast Greenland and implications for ice sheet mass changes, *J. Geophys. Res*., **115**, F03026.

Murray, T., Strozzi, T., Luckman, A., Pritchard, H., and Jiskoot, H., (2002), Ice dynamics during a surge of Sortebrae, East Greenland, *Ann. Glac*., **34**(1), 323-329.

Myers, P., Kulan, N., and Ribergaard, M.H., (2007), Irminger Water variability in the West Greenland Current, *Geophys. Res. Lett*., **34**, L17601.

Nick, F., Vieli, A., Howat, I., and Joughin, I., (2009), Large-scale changes in Greenland outlet glacier dynamics triggered at the terminus, *Nature Geosci*., **2**, 110-114.

Pritchard, H., Arthern, R., Vaughan, D., and Edwards, L., (2009), Extensive dynamic thinning on the margins of the Greenland and Antarctic ice sheets, *Nature*, **461**, 971-975.

Ramillien, G., Lombard, A., Cazenave, A., Ivins, E.R., Llubes, M., Remy, F., and Biancale, R., (2006), Interannual variations of the mass balance of the Antarctica and Greenland ice sheets from GRACE, *Global Planetary Change*, **53**, 198–208.

Rignot, E., Koppes, M., and Velicogna, I., (2010), Rapid submarine melting of the calving faces of West Greenland glaciers, *Nature Geosci.,* **3**, 765.

Rignot, E., Box, J.E., Burgess, E., and Hanna, E., (2008), Mass balance of the Greenland ice sheet from 1958 to 2007, *Geophys. Res. Lett*., **35**, L20502.

Rignot, E. and Kanagaratnam, P., (2006), Changes in the Velocity Structure of the Greenland Ice Sheet, *Science*, **311**, 986-990.

Rignot, E., Braaten, D., Gogineni, S., Krabill, W., and McConnell, J.R., (2004), Rapid ice discharge from southeast Greenland glaciers, *Geophys. Res. Lett*., **31**, L10401.

Seale, A., Christofferson, P., Mugford, R.I., and O'Leary, M., (2011), Ocean forcing of the Greenland Ice Sheet: Calving fronts and patterns of retreat identified by automatic satellite monitoring of eastern outlet glaciers, *J. Geophys. Res.,* **116**, F03013.

Stearns, L. and G. Hamilton (2007), Rapid volume loss from two East Greenland outlet glaciers quantified using repeat stereo satellite imagery, *Geophys. Res. Lett*., **34**, L05503.

Straneo, F., Hamilton, G., Sutherland, D., Stearns, L., Davidson, F., Hammill, M., Stenson, G., Rosing-Asvid, A., (2010), Rapid circulation of warm subtropical waters in a major glacial fjord in East Greenland, *Nature Geosci.*, **3**, 764.

Tapley, B., Bettadpur, S., Watkins, M., and Reigber, C., (2004), The gravity recovery and climate experiment: Mission overview and early results, *Geophys. Res. Lett*., **31**, L09607.

Thierry, V., de Boisséson, E., and Mercier, H., (2008), Interannual variability of the Subpolar Mode Water properties over the Reykjanes Ridge during 1990-2006, *J. Geophys. Res*., **113**, C04016.

Thomas, R., Frederick, E., Krabill, W., Manizade, S., and Martin, C., (2006), Progressive increase in ice loss from Greenland, *Geophys. Res. Lett*., **33**, L10503.

Thomas, R.H. (2004), Force-perturbation analysis of recent thinning and acceleration of Jakobshavn Isbrae, Greenland, *J. Glaciol*., **50**, 57-66.

van den Broeke, M., Bamber, J., Ettema, J., Rignot, E., Schrama, E., van de Berg, W., van Meijgaard, E., Velicogna, I., and Wouters, B., (2009), Partitioning Recent Greenland Mass Loss, *Science*, **326**, 984-986.

Velicogna, I. (2009), Increasing rates of ice mass loss from the Greenland and Antarctic ice sheets revealed by GRACE, *Geophys. Res. Lett*., **36**, L19503.

Velicogna, I., and J. Wahr (2006), Acceleration of Greenland ice mass loss in spring 2004, *Nature*, **443**, 329-331.

Weidick, A. (1988), Surging glaciers in Greenland: a status. *Grønl. Geol. Undersøgelse, Rapp*. **140**, 106-110.

Zwally, H.J., Abdalati, W., Herring, T., Larson, K., Saba, J., and Steffen, K., (2002), Surface Melt-Induced Acceleration of Greenland Ice-Sheet Flow, *Science*, **297**, 218-222.

Zwally, H.J, Li, J., Brenner, A.C., Beckley, M., Cornejo, H.G., DiMarzio, J., Giovinetto, M.B., Neumann, T.A., Robbins, J., Saba, J.L., Yi, D., and Wang, W., (2011), Greenland ice sheet mass balance: distribution of increased mass loss with climate warming; 2003-07 versus 1992-2002, *J. Glaciol*., **57**, 88-102.

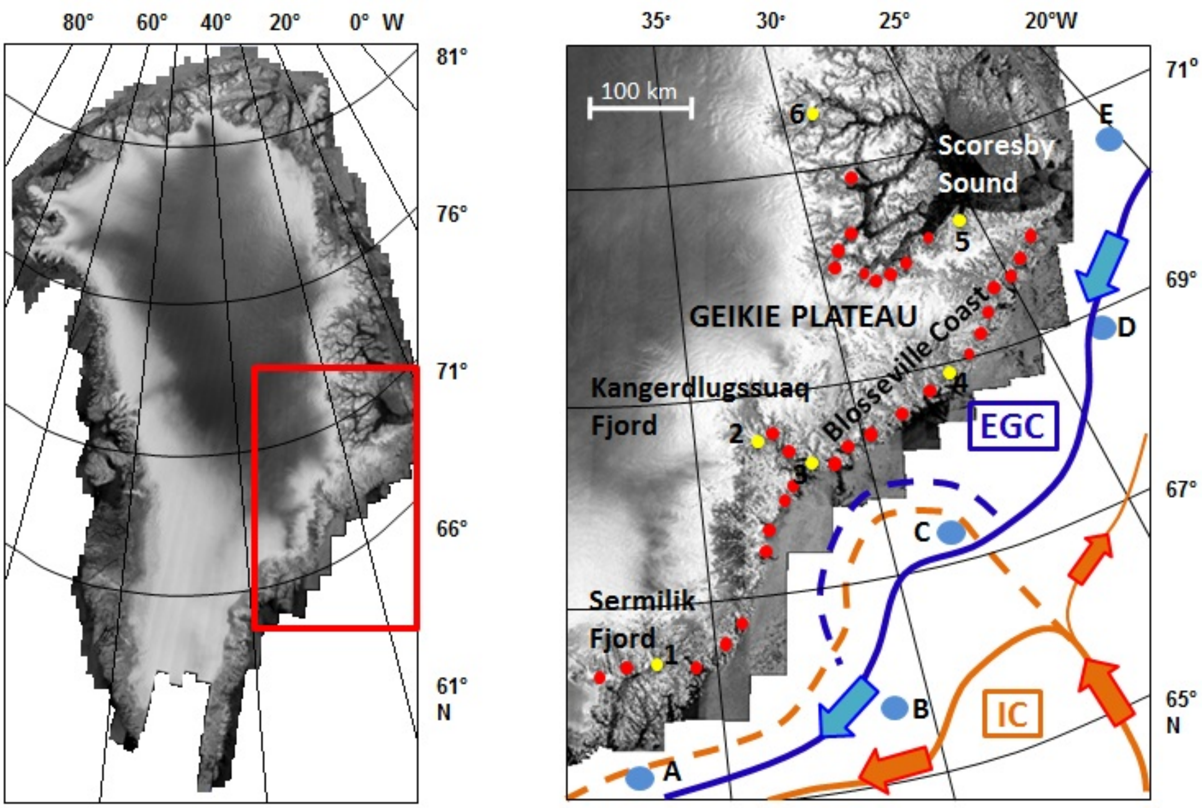

Figure 1: RADARSAT mosaic showing area of study; including Sermilik Fjord, Kangerdlugssuaq Fjord, Geikie Plateau, Blosseville Coast, and Scoresby Sound; specific glaciers, sea surface temperature points, and relevant ocean currents in the region of study; red dots indicate each glacier; glaciers discussed in detail in the text are indicated by yellow dots and numerals (1 = Midgard; 2 = Kangerdlugssuaq; 3 = Frederiksborg; 4 = Sortebrae; 5 = Sydbrae; 6 = Daugaard-Jensen); blue dots indicate sea surface temperature observation points (A through E); “IC” and the orange lines depict the Irminger Current; “EGC” and the blue lines depict the East Greenland Current; dotted lines represent variations in each ocean current.

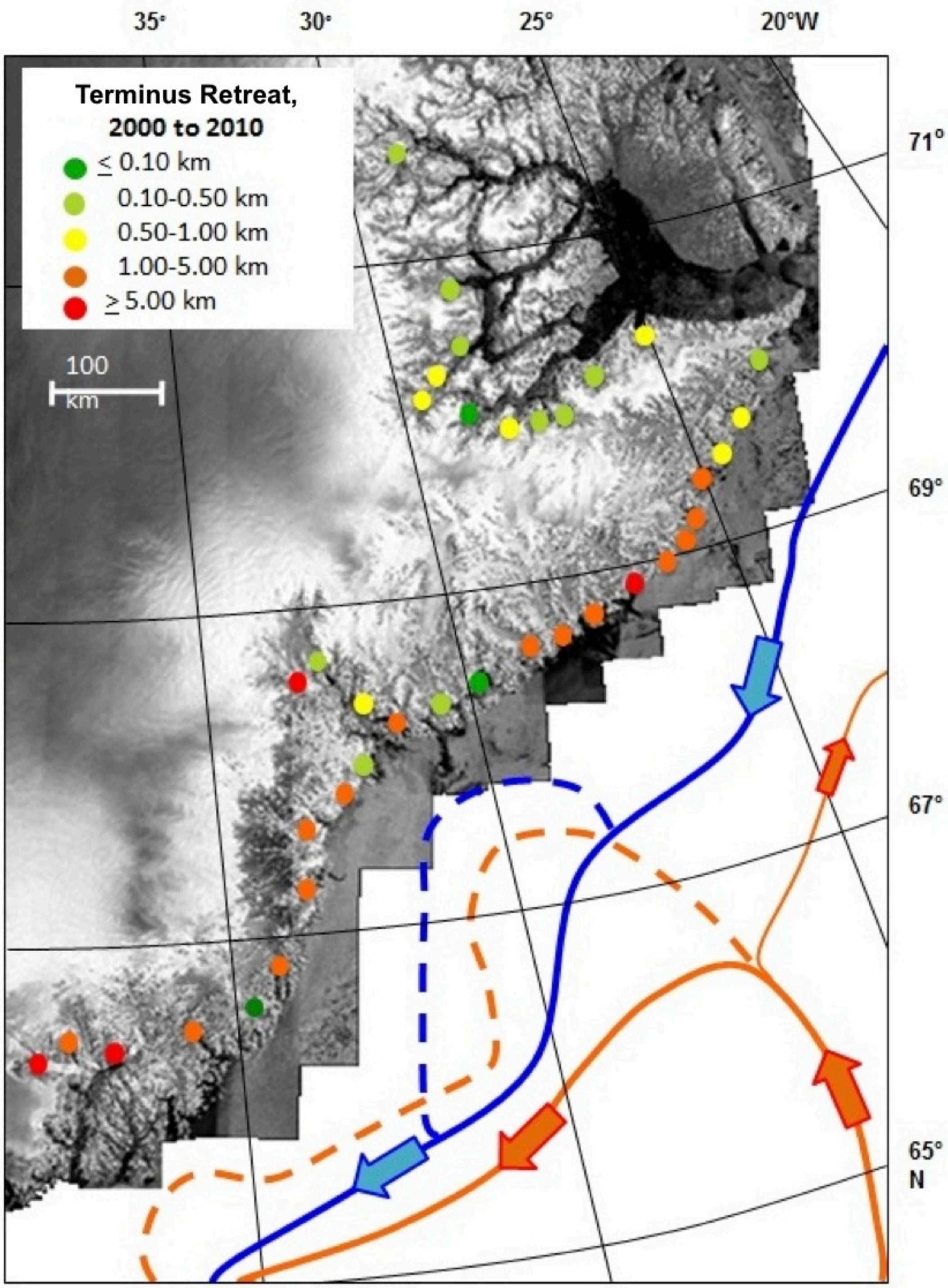

Figure 2: Change in front position (2000-2010) for all marine-terminating outlet glaciers in this analysis. Circles indicate the location of each glacier and colors indicate magnitude of retreat.

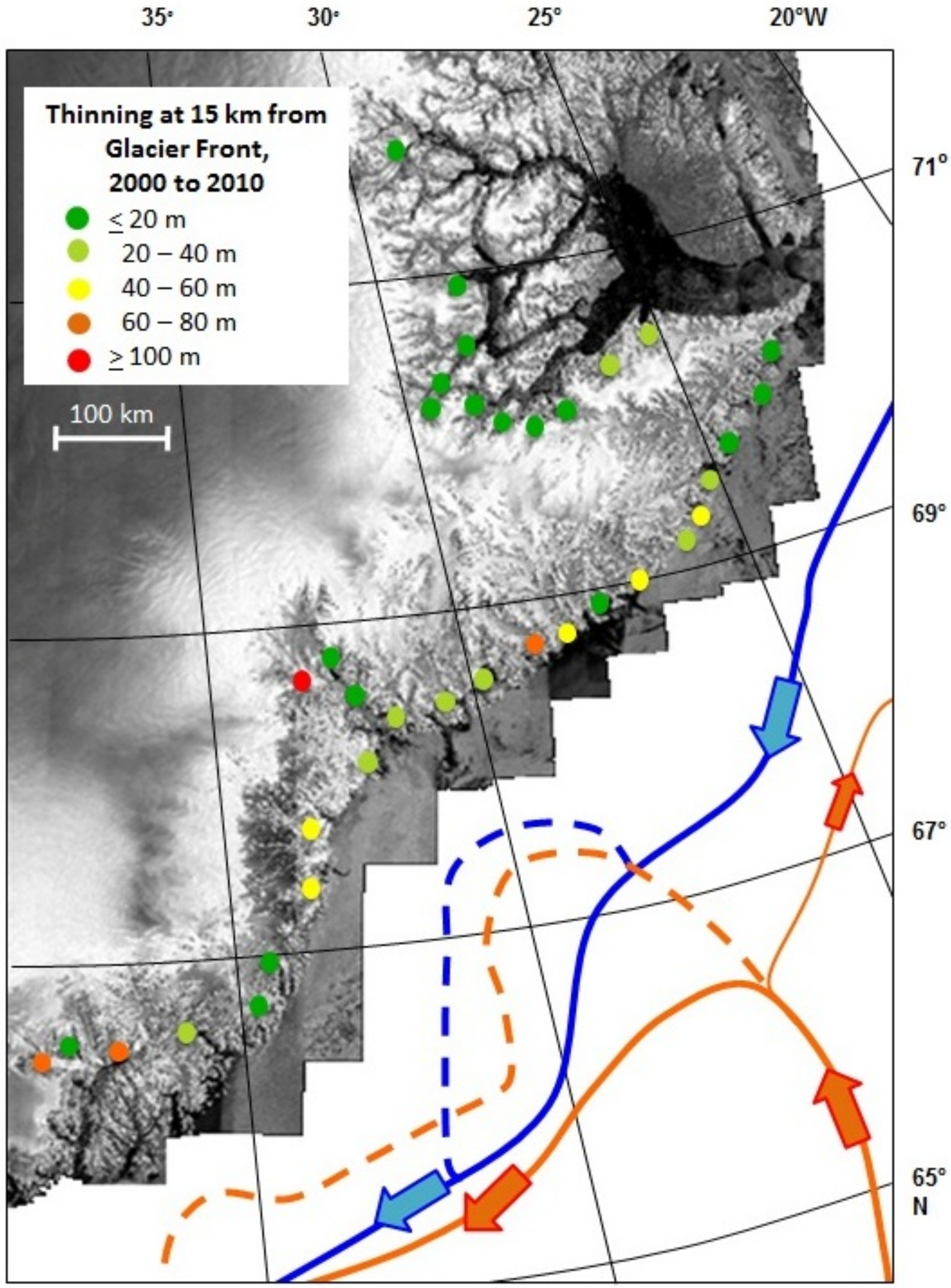

Figure 3: Change in surface elevation (all values negative) (2000-2010) for all marine-terminating outlet glaciers in this analysis. Thinning measured at 15 km from most retreated front position. Circles indicate the location of each glacier and colors indicate magnitude of thinning.

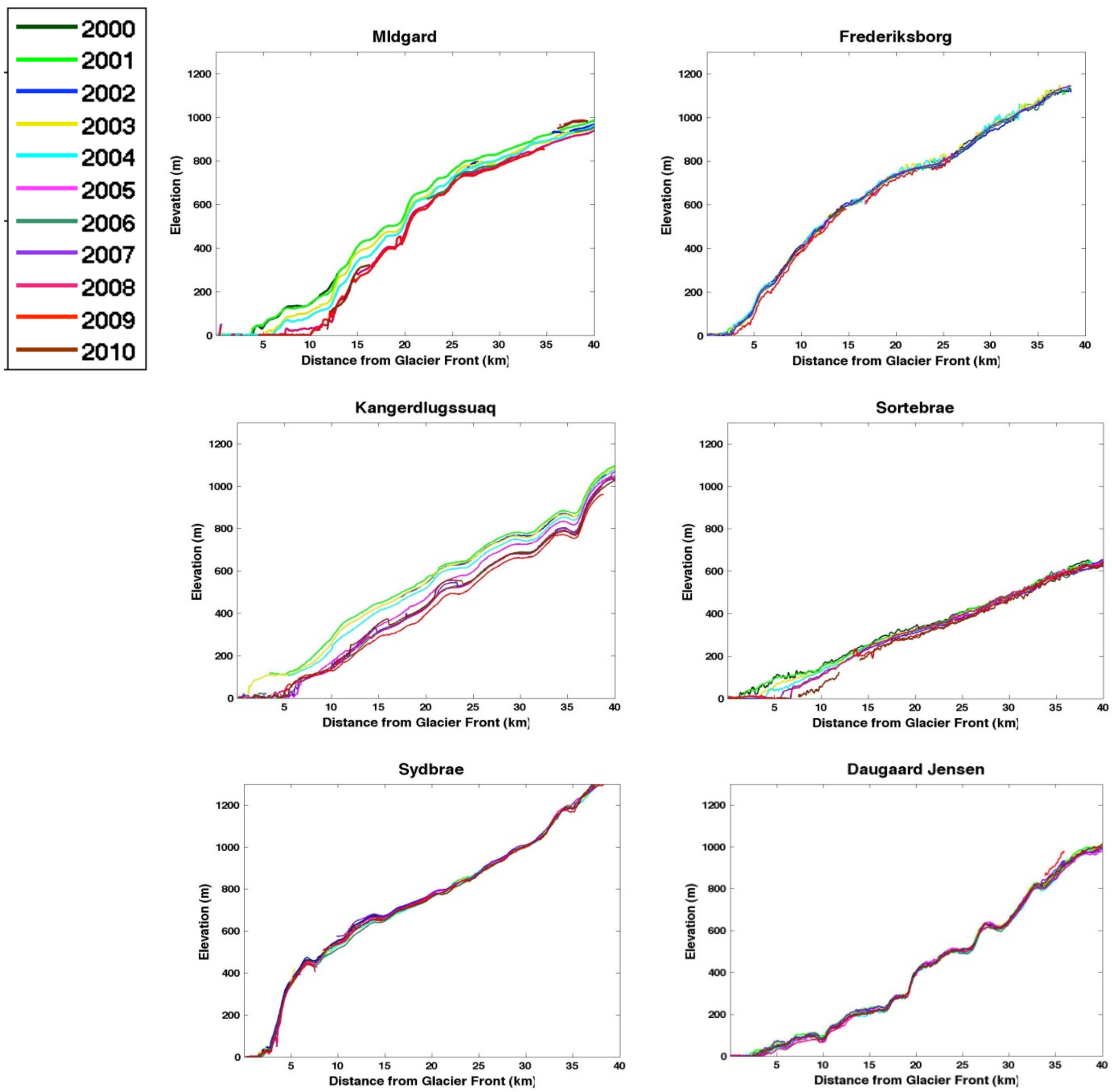

Figure 4: Elevation profiles for six (6) marine-terminating outlet glaciers in the dataset. Latitude increases from top to bottom, starting with Midgard Glacier (66°26’N, 36°45’W) to Daugaard Jensen Glacier (71°54’N, 28°36’W). Elevation profiles show annual average elevation from the terminus upglacier to the accumulation zone for each glacier.

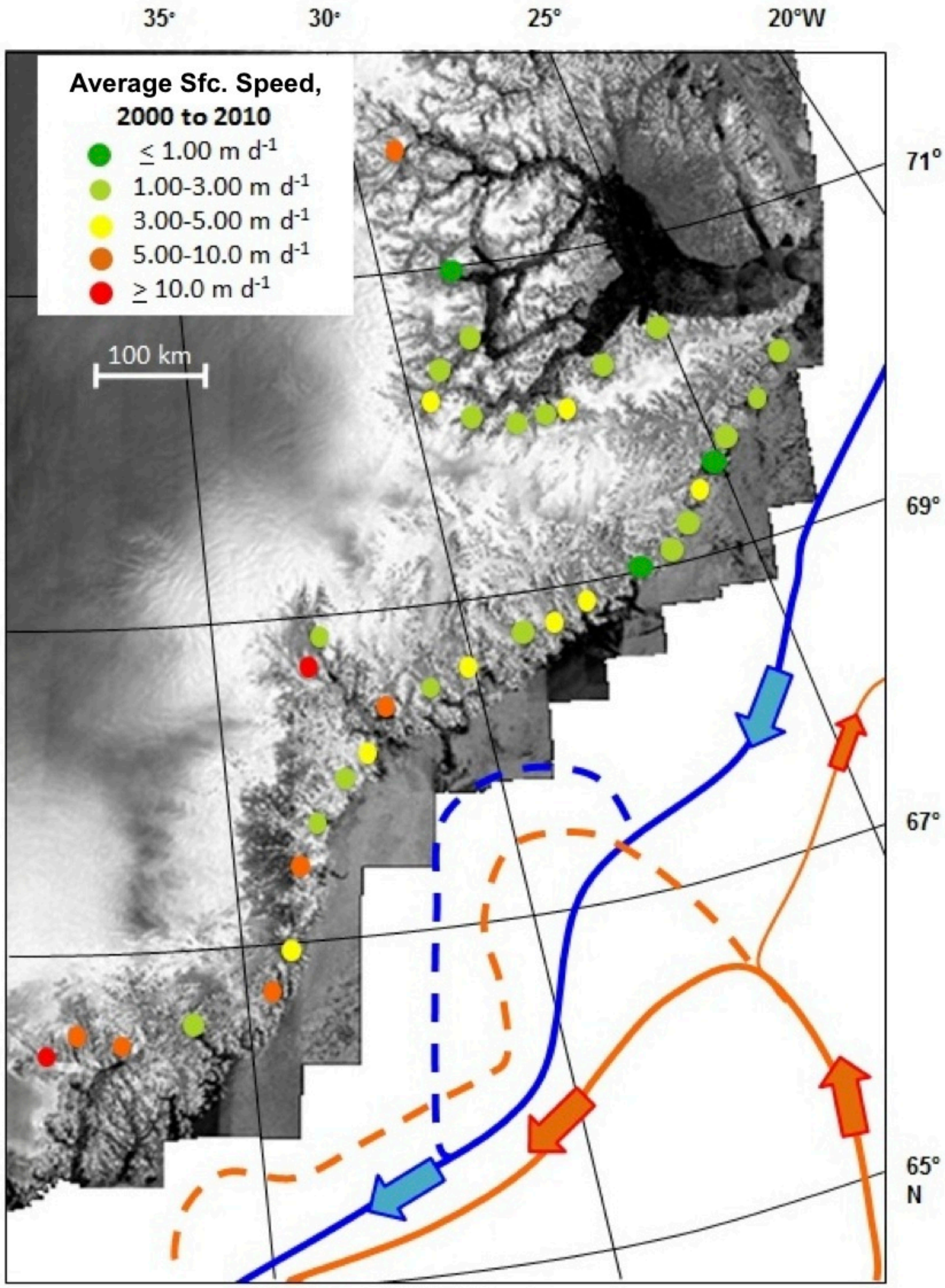

Figure 5: Average surface speeds (in m d^{-1}) for all marine-terminating glaciers in the data set. Circles indicate the location of each glacier and colors indicate magnitude of glacier speed.

Figure 6: Landsat-7 ETM+ image from 2000 showing progression of retreat in 2005 and 2010; Midgard has retreated roughly 9 km since 2000.

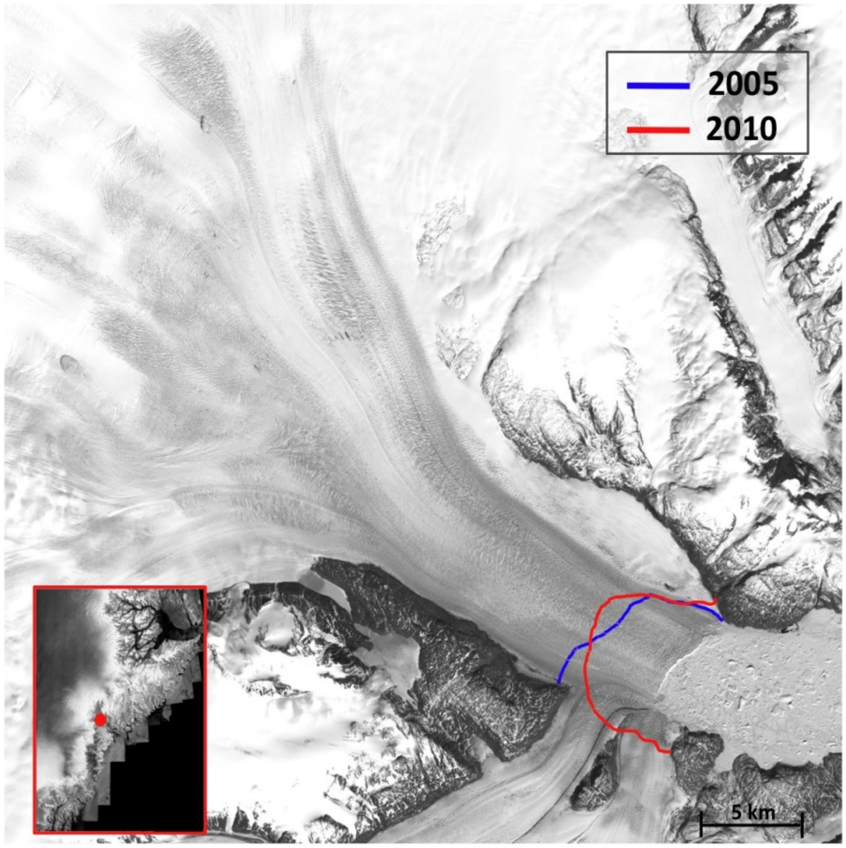

Figure 7: Landsat-7 ETM+ image from 2000 showing progression of retreat in 2005 and 2010; Kangerdlugssuaq has retreated roughly 7 km since 2000.

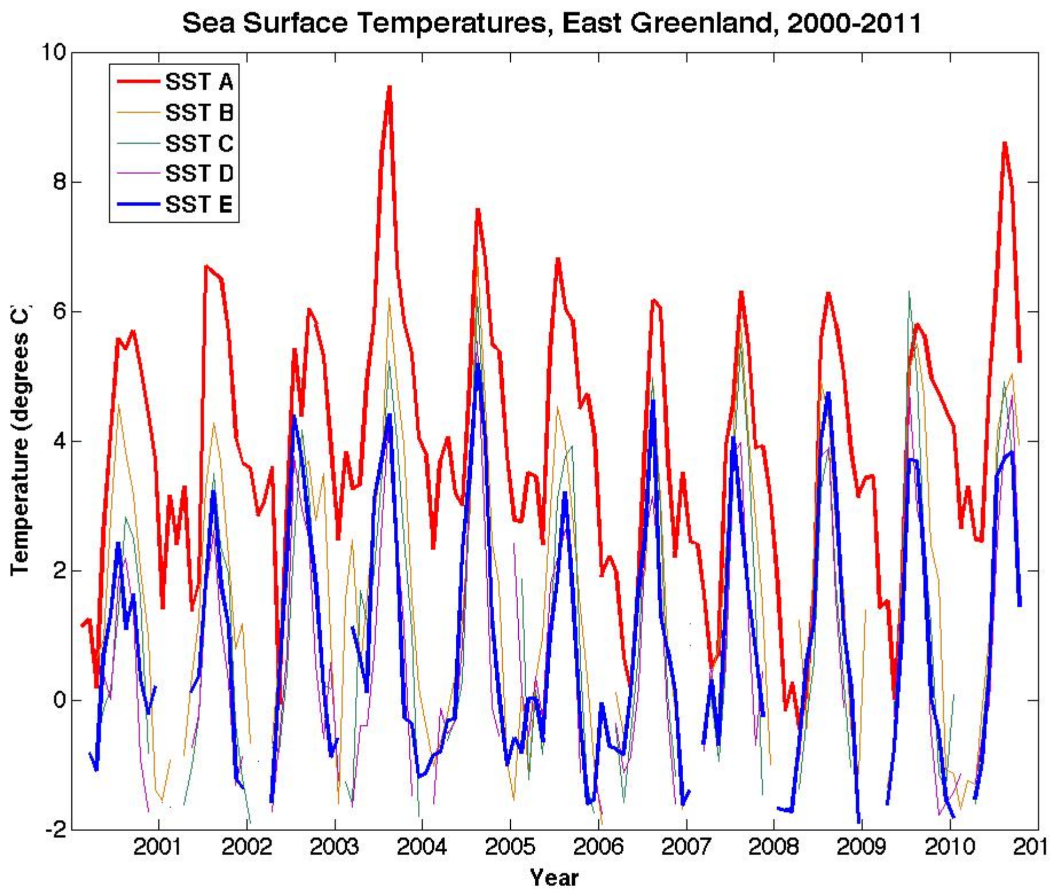

Figure 8: Sea surface temperatures (SSTs) derived from MODIS data from 2000 to 2010 from five sites off of the central east Greenland coast; see figure 1 for SST measurement point locations. Of note is the clear spike in SSTs in 2003, which corresponds to a period of anomalously warm atmospheric temperatures as well (Howat et al., 2008a).